Check for updates

Investigating nonflow contribution on elliptic flow in p-Pb collisions with the AMPT model

Ning Yu[1,2,3], Zuman Zhang[1,2,3]* and Meimei Zhang[1,4]

[1]School of Physics and Mechanical Electrical and Engineering, Hubei University of Education, Wuhan, China, [2]Institute of Theoretical Physics, Hubei University of Education, Wuhan, China, [3]Key Laboratory of Quark and Lepton Physics (MOE), Central China Normal University, Wuhan, China, [4]Center for Astronomy and Space Sciences, China Three Gorges University, Yichang, China

This study investigates the subtraction of nonflow contributions in heavy-ion collisions using the multiphase transport (AMPT) model, focusing on unidentified charged trigger particles and various species of charged associated particles, including pions, kaons, protons, and antiprotons. The analysis centers on elliptic flow (v_2) measurements in proton-lead (p-Pb) collisions at a center-of-mass energy of $\sqrt{s_{NN}} = 5.02$ TeV, within the transverse momentum range of $0.3 < p_T < 4$ GeV/c. We aim to evaluate the influence of nonflow sources, such as jet correlations and resonance decays, particularly in small collision systems. To reduce nonflow effects, we subtract the per-trigger yield distribution from peripheral p-Pb or proton-proton collisions at the same energy. Our results indicate that nonflow contributions in central collisions exhibit minimal dependence on the subtraction of per-trigger yields from peripheral p-Pb or pp collisions. We can find the second-order coefficients for pions and kaons are comparable, while v_2^p is smaller at low p_T and larger at high p_T compared to v_2^π, with a crossing observed around 2 GeV/c. A comparison with experimental data from p-Pb collisions at $\sqrt{s_{NN}} = 5.02$ TeV is also presented. PACS 25.75. LdCollective flow · 24.10. LxMonte Carlo simulations (including hadron and parton cascades and string breaking models).

1 Introduction

In the field of high-energy heavy-ion collisions, one of the primary objectives is to explore the properties of the quark-gluon plasma (QGP), a state of matter characterized by extremely high energy density and temperature [1, 2]. A crucial observable in understanding the QGP is the azimuthal anisotropy of final state particles, which serves as a sensitive probe for the transport properties and collective behavior of this deconfined medium [3]. The elliptic flow (v_2), in particular, is a key observable that reflects the collective motion of the medium and is typically extracted via a Fourier expansion of the azimuthal distribution of emitted particles in transverse momentum space. The second-order coefficient of this expansion, v_2, provides insight into the anisotropic pressure gradients within the QGP and its hydrodynamic response to initial geometry fluctuations [3, 4]. The study of elliptic flow is a crucial aspect of high-energy heavy-ion collision research, as it provides deep insights into the formation and characteristics of the QGP.

To further comprehend the influence of cold nuclear matter (CNM) effects on the interpretation of measurements in heavy-ion collisions, we have extended our investigation to smaller collision systems, such as proton-nucleus or deuteron-nucleus (p(d)+A) collisions. These systems serve as an essential tool for isolating CNM effects from those arising from QGP formation. Our study focuses on several key CNM effects, including modifications to parton distribution functions (PDFs) [5], k_T broadening [6], and partonic energy loss in cold nuclear matter [7]. Experiments involving high-multiplicity p + A collisions at $\sqrt{s_{NN}}$ = 5.02 TeV, conducted by the ALICE, ATLAS, and CMS collaborations in the midrapidity region [8–13], and by the LHCb collaboration at forward rapidity [14], revealed long-range structures in two-particle azimuthal correlations. These structures were associated with a positive elliptic flow coefficient, v_2, for hadrons, similar to the signals observed in larger systems. Additionally, at lower beam energies, similar long-range correlations have been observed in p-Pb collisions [15–17] and ^{3}He-Au collisions [18] at the Relativistic Heavy Ion Collider (RHIC) by the PHENIX and STAR collaborations.

It is essential to account for nonflow effects, which arise from sources unrelated to collective motion, such as jets, resonance decays, and dijet production. Various strategies have been developed to suppress or eliminate these nonflow contributions. In small collision system experiments, these effects are typically reduced by applying a pseudorapidity gap between paired particles or by subtracting correlations measured in low-multiplicity events or pp collisions [9, 19, 20]. A standard template fit procedure [21] is then employed to isolate the long-range correlations. In the LHC experimental analyses, nonflow contributions have not been consistently evaluated using both methods within the same collision system. Therefore, we analyze the transverse momentum (p_T) dependence of anisotropic flow (v_2) in p-Pb collisions at $\sqrt{s_{NN}}$ = 5.02 TeV by employing the multiphase transport (AMPT) model [22]. This allows us to investigate nonflow subtraction using both peripheral p-Pb and pp collisions.

p-Pb collisions occur at $\sqrt{s_{NN}}$ = 5.02 TeV and have higher collision energies than d-Au collisions (usually conducted at RHIC 200 GeV), which can produce stronger collective flows (such as elliptical flows v_2), making it clearer to distinguish between nonflow contributions and collective motion. p-Pb collisions have more complex nonflow contributions than pp collisions, including jet correlations, resonance decays, and dijet production, which are usually smaller in pp collisions.

This paper begins with a introduction to the AMPT model and its relevance to our study. Next, we describe the methodology used to subtract nonflow contributions, emphasizing the differences between the two subtraction methods. Finally, the results are presented, along with a discussion and conclusion.

2 Event generation and definition of anisotropic flow

2.1 A multi-phase transport (AMPT) model

The AMPT model [22] is a hybrid transport model widely employed to investigate collective behavior in heavy-ion collisions.

It integrates four key components: (1) the generation of initial conditions, (2) partonic interactions, (3) the conversion from partonic matter to hadronic matter, and (4) hadronic interactions.

The Lund string fragmentation function, a key component in the initial stage, is determined by the parameters a and b in HIJING [23]. It is expressed as $f(z) \propto z^{-1}(1-z)^a \exp(-bm_\perp^2/z)$, where z represents the light-cone momentum fraction of the produced hadron relative to the fragmenting string, and $m_\perp$ is the transverse mass of the hadron.

The Zhang's Parton Cascade (ZPC) model [24] is used to simulate the evolution of the partonic phase, where parton-parton scattering occurs. The cross section for these scatterings is approximated as $\sigma \approx \frac{9\pi\alpha_s^2}{2\mu^2}$, where α_s is the strong coupling constant and μ is the Debye screening mass, which accounts for medium-induced screening effects in the partonic system. ZPC tracks the evolution of partons until they cease to interact, marking the end of the partonic phase.

After parton interactions end in ZPC, the hadronization process begins, governed by the quark coalescence model. In this process, quarks in close proximity in coordinate space combine to form hadrons. The coalesced hadrons then enter the hadronic phase, where their subsequent interactions are handled by the relativistic transport (ART) model [25]. The ART model simulates hadron-hadron scatterings using input cross sections for various channels.

In this work, we employ the string melting version of the AMPT model. We conducted approximately 10 million AMPT events for p-Pb collisions at $\sqrt{s_{NN}}$ = 5.02 TeV, as well as for pp collisions at $\sqrt{s}$ = 5.02 TeV. Each event required approximately 0.1 s of CPU time, amounting to a total computational effort of 280 CPU hours for the entire data sample. The event centrality in p + Pb collisions was determined using the impact parameter b from AMPT-generated events.

For the analysis, we selected central and peripheral event samples, corresponding to 0%–20% and 60%–100% collision centrality intervals, respectively. These samples were used to study the elliptic flow (v_2) distributions of unidentified particles, including charged particles, pions, kaons, protons, and antiprotons.

2.2 Definition of anisotropic flow

Typically, the magnitude of azimuthal anisotropies in heavy-ion collisions is quantified through a Fourier decomposition of the particle azimuthal distribution. This distribution, as a function of the azimuthal angle (φ) and transverse momentum (p_T) of produced particles, captures the anisotropic flow patterns generated in the collision process. The azimuthal distribution can be expressed as:

$$\frac{d^2N}{dp_T d\varphi} = \frac{1}{2\pi}\frac{dN}{dp_T}\left(1 + 2\sum_{n=1}^{\infty} v_n(p_T)\cos[n(\varphi - \Psi_n)]\right), \quad (1)$$

where the anisotropy of produced particles is defined by the Fourier coefficients v_n [26, 27] and the azimuthal angle of the symmetry plane for the nth harmonic is denoted by Ψ_n. The largest contribution to the asymmetry of collisions is provided by the second Fourier coefficient v_2 referred to as elliptic flow [3, 26].
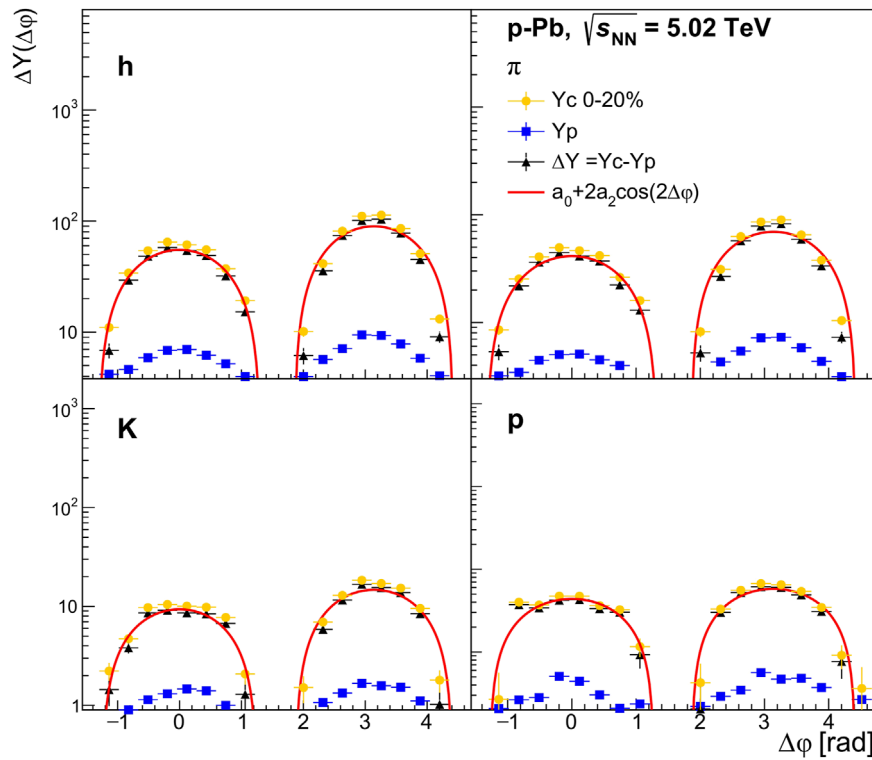
FIGURE 1
Unidentified charged particles, pions, kaons, protons azimuthal conditional yields $Y(\Delta\phi)$ for 0%−20% most central ($Y_c(\Delta\phi)$, orange circles) and 60%−100% peripheral ($Y_p(\Delta\phi)$, blue squares) collisions with $0.8 < |\Delta\eta| < 1.6$ on the near side ($|\Delta\phi| < \pi/2$) and $|\Delta\eta| < 1.6$ on the away side ($\pi/2 < |\Delta\phi| < 3\pi/2$). Each particle pair is chosen from the same p_T interval, $1.25 < p_T < 1.5$ GeV/c. Difference $\Delta Y(\Delta\phi)$ between most central and peripheral p-Pb collisions ($\Delta Y_{cp}(\Delta\phi) = Y_c(\Delta\phi) - Y_p(\Delta\phi)$, black triangle-ups), which is fit to $a_0 + 2a_2 \cos(2\Delta\phi)$(red curve), where a_0 and a_2 are computed from the AMPT events.

3 Nonflow contribution subtraction method

The method of extracting azimuthal anisotropy using two-particle correlations has been extensively discussed in previous studies [8–14, 28–31]. In this approach, the correlation between two particles, often referred to as the trigger and associated particle, is measured as a function of their azimuthal angle difference, $\Delta\phi$, and their pseudorapidity difference, $\Delta\eta$. The azimuthal angle difference is defined within the range $-\pi/2 < \Delta\phi < 3\pi/2$, while $\Delta\eta$ represents the separation in pseudorapidity.

In the analysis, the trigger particles are typically charged particles, and correlations are examined with various species of charged associated particles, including unidentified charged particles, pions, kaons, protons, and antiprotons. These are denoted by combinations such as h-h (charged-charged), h-π (charged-pion), h-K (charged-kaon), and h-p (charged-proton), where the first particle is the trigger and the second is the associated particle.

For this study, we follow the analysis procedures from experiments conducted at ALICE [11]. Specifically, in AMPT simulations, charged hadrons within a transverse momentum range of $0.3 < p_T < 4$ GeV/c are selected. Each particle pair is chosen from the same p_T interval, ensuring that both particles share similar transverse momenta.

To suppress short-range correlations and focus on collective flow, pairs of particles are required to have a pseudorapidity separation within certain ranges. For near-side correlations ($-\pi/2 < |\Delta\phi| < \pi/2$), pairs are restricted to $0.8 < |\Delta\eta| < 1.6$, while for away-side correlations ($\pi/2 < |\Delta\phi| < 3\pi/2$), the separation is $|\Delta\eta| < 1.6$.

The correlation is expressed in terms of Y, the associated yield per trigger particle defined as:

$$Y = \frac{1}{N_{\text{trig}}} \frac{dN_{\text{assoc}}}{d\Delta\phi}, \qquad (2)$$

where N_{trig} is the total number of trigger particles in the event class and p_T interval, N_{assoc} is the total number of associated particles in the event class and p_T interval.

We apply zero-yield-at-minimum (ZYAM) method [32] to estimate and subtract the background contribution in the analysis of azimuthal correlations. The ZYAM method operates on the assumption that the number of correlated particle pairs reaches zero at the minimum of the correlation function. This background level is extracted for central, mid-central, peripheral, and pp collision samples by fitting the conditional yields to a function composed of a constant pedestal term and two Gaussian peaks, centered at $\Delta\phi = 0$ and $\Delta\phi = \pi$ to account for near-side and away-side correlations, respectively. The minimum value of the fit, denoted as b_{ZYAM}, is then subtracted from the measured conditional yields to obtain the background-corrected distribution: $Y(\Delta\phi) = \frac{1}{N_{\text{trig}}} \frac{dN_{\text{assoc}}}{d\Delta\phi} - b_{\text{ZYAM}}$,
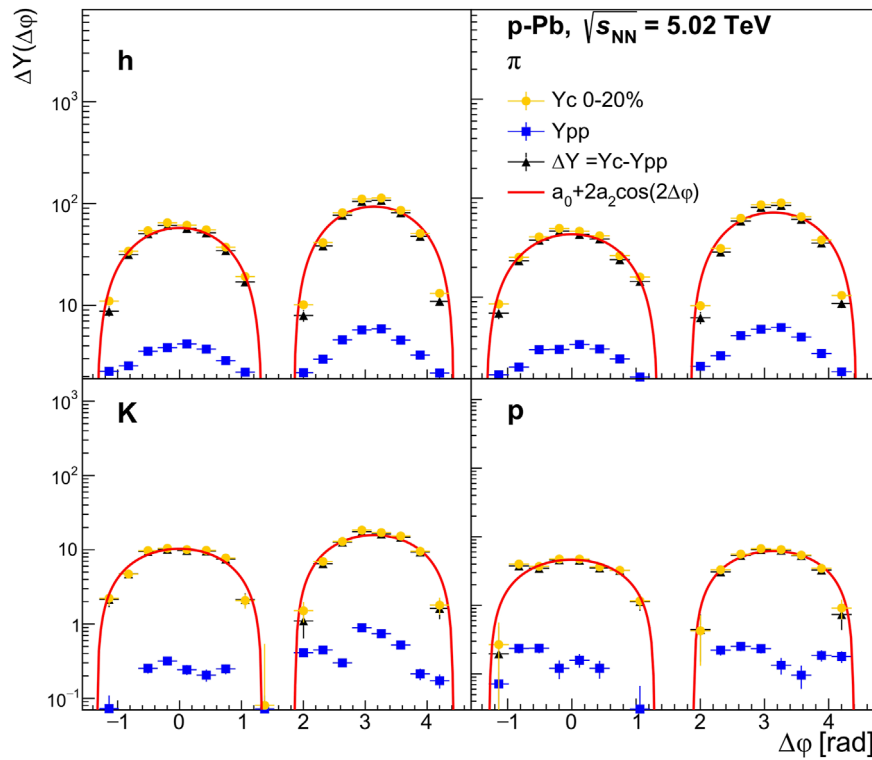
FIGURE 2
Unidentified charged particles, pions, kaons, protons azimuthal conditional yields $Y(\Delta\varphi)$ for 0%−20% most central ($Y_c(\Delta\varphi)$, orange circles) and pp ($Y_{pp}(\Delta\varphi)$, blue squares) collisions with $0.8 < |\Delta\eta| < 1.6$ on the near side ($|\Delta\phi| < \pi/2$) and $|\Delta\eta| < 1.6$ on the away side ($\pi/2 < |\Delta\phi| < 3\pi/2$). Each particle pair is chosen from the same p_T interval, $1.25 < p_T < 1.5$ GeV/c. Difference $\Delta Y(\Delta\varphi)$ between most central p-Pb collisions and pp collisions ($\Delta Y_{cpp}(\Delta\phi) = Y_c(\Delta\phi) − Y_{pp}(\Delta\phi)$, black triangle-ups), which is fit to $a_0 + 2a_2\cos(2\Delta\phi)$(red curve), where a_0 and a_2 are computed from the AMPT events.

where $Y(\Delta\phi)$ represents the corrected yield of associated particles per trigger particle as a function of the azimuthal angle difference $\Delta\phi$, N_{trig} is the number of trigger particles, and b_{ZYAM} is the background level at the correlation minimum.

The conditional yields for different centrality classes are denoted as $Y_c(\Delta\phi)$ for central collisions, $Y_p(\Delta\phi)$ for peripheral collisions, and $Y_{pp}(\Delta\phi)$ for pp collisions. To investigate the impact of centrality-dependent correlations and eliminate centrality-independent effects (such as those arising from jets, resonance decays, and other nonflow contributions), we compute the differences between the yields in different centrality classes as follows: $\Delta Y_{cp}(\Delta\phi) = Y_c(\Delta\phi) − Y_p(\Delta\phi)$ (central vs peripheral), $\Delta Y_{cpp}(\Delta\phi) = Y_c(\Delta\phi) − Y_{pp}(\Delta\phi)$ (central vs pp).

Fourier coefficients can be extracted from the $\Delta\phi$ projection of the per-trigger yield by a fit with:

$$\frac{1}{N_{trig}}\frac{dN_{assoc}}{d\Delta\phi} = a_0 + \sum_{n=1}^{3} 2a_n\cos(n\Delta\phi) \qquad (3)$$

To quantify the relative amplitude of the azimuthal modulation, we define

$$c_n = a_n / (b^c_{ZYAM} + a_0), \qquad (4)$$

where b^c_{ZYAM} is b_{ZYAM} in central events [32], a_0 and a_2 are computed from the AMPT events.

The method using two-particle correlations to the $v^i_n\{2PC\}$ coefficient of order n for a particle i (out of h, π, K, p) is defined as [11]:

$$v^i_n\{2PC\} = c^{h-i}_n / \sqrt{c^{h-h}_n} \qquad (5)$$

4 Results and discussions

From Equation 2, the charged particles (h, π, K, p) conditional yields $Y_c(\Delta\phi)$, $Y_p(\Delta\phi)$ and $Y_{pp}(\Delta\phi)$(0%−20% most central, peripheral and pp collisions events, respectively) are shown in Figures 1, 2, along with their difference $\Delta Y_{cp}(\Delta\phi) = Y_c(\Delta\phi) − Y_p(\Delta\phi)$ and $\Delta Y_{cpp}(\Delta\phi) = Y_c(\Delta\phi) − Y_{pp}(\Delta\phi)$ are expressed as subtracting the per-trigger yield distribution in peripheral p-Pb collisions at $\sqrt{s_{NN}} = 5.02$ TeV or pp collisions at $\sqrt{s} = 5.02$ GeV, respectively. It is worth noting that any signal in the peripheral events and pp events is subtracted from the signal in the central events. For $\Delta\phi$ near 0 and π, $Y_c(\Delta\phi)$ is significantly larger than $Y_p(\Delta\phi)$ and $Y_{pp}(\Delta\phi)$.

We discover that the distinction with 0%−20% most central, 60%−100% peripheral collisions and pp collisions are well described by Equation 3 as demonstrated in Figures 1, 2. The charged particles coefficients a_n are computed from the $\Delta Y(\Delta\phi)$ distributions as:
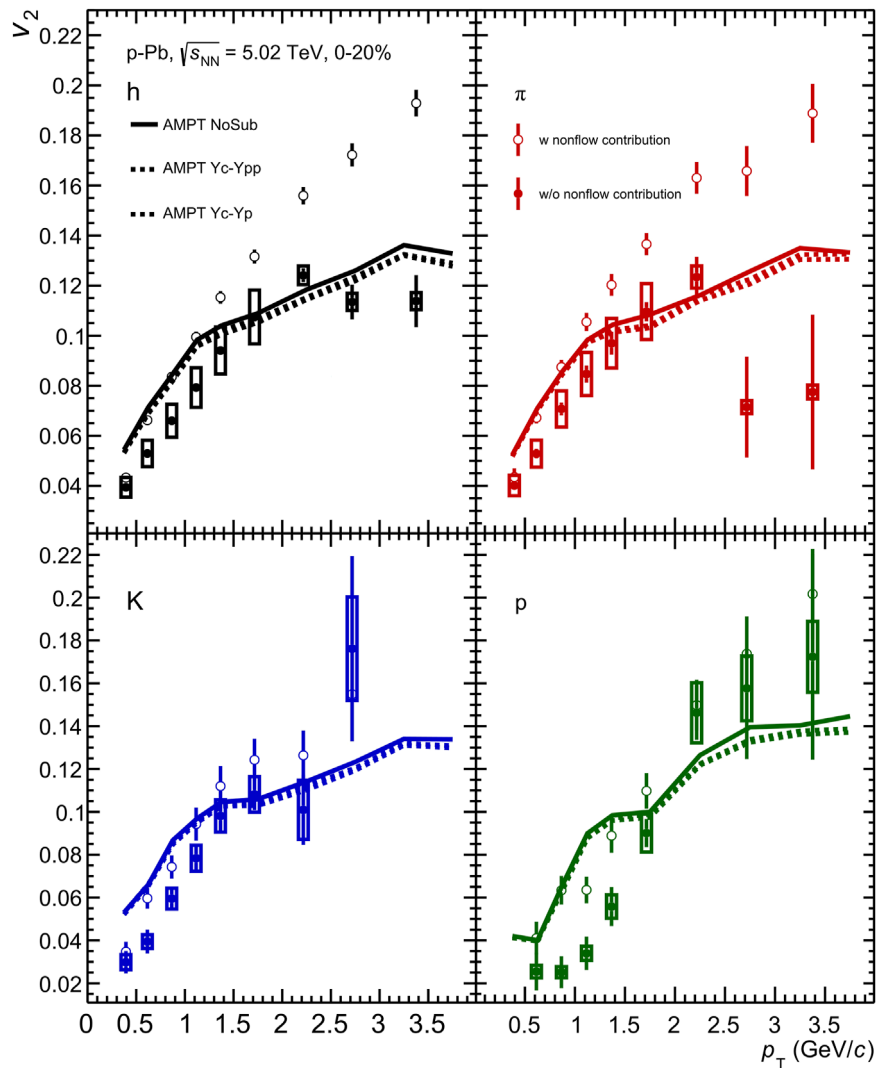
FIGURE 3
In two-particle correlation both particles are taken from the same p_T interval (p_T). With $0.8 < |\Delta\eta| < 1.6$ on the near side ($|\Delta\phi| < \pi/2$) and $|\Delta\eta| < 1.6$ on the away side ($\pi/2 < |\Delta\phi| < 3\pi/2$). The charged particles (h, π, K, p) elliptic flow v_2 of the 0%−20% most central p-Pb collision excess as a function of associated particle p_T. The solid line is for v_2 of the 0%−20% most central p-Pb collisions with nonflow effects. The nonflow effects for 0%−20% most central p-Pb collisions reduced by subtracting the per-trigger yield distribution in peripheral p-Pb collisions (short dash-dotted line) or pp collisions (long dash-dotted line). The v_2 of the central p-Pb collision with and without nonflow contribution in the data is also shown (circles) from Ref. [11].

$a_n = \langle \Delta Y(\Delta\phi) \cos(n\Delta\phi) \rangle$. The bracket $\langle \dots \rangle$ denotes an average over particles in the event sample with $\Delta\phi$.

From Equation 5, charged particles (h, π, K, p) v_2 is shown as a function of associated p_T in Figure 3 for central (0%−20%) p-Pb collisions. We can observe the charged particles v_2 value increase with p_T distribution, this is because at higher p_T, the particles are more affected by reflecting the initial spatial anisotropy of the collision geometry. The presence of nonflow effects is shown when comparing the solid line (with nonflow effects) to the short dash-dotted and long dash-dotted (without nonflow effects). In these comparisons, the solid line is consistently higher. Specifically, the black line represents unidentified charged particles, the red line corresponds to pions, the blue line to kaons, and the green line to protons. For 0%−20% of the most central p-Pb collisions, the nonflow effects were reduced by subtracting the per-trigger

yield distribution observed in peripheral p-Pb collisions or in pp collisions. The results show that this subtraction leads to very similar outcomes in both cases. This suggests that the nonflow effects, such as those caused by jet correlations and resonance decays, in the 0%−20% most central p-Pb collisions do not exhibit a strong dependence on whether the subtraction is done using peripheral p-Pb or pp collision events. This suggests that nonflow effects (such as jet correlations and resonance decays) are not strongly dependent on whether peripheral p-Pb or pp collisions are used as a reference. With nonflow effects, the v_2 of charged particles (including unidentified particles, pions, kaons, protons, and antiprotons) from AMPT simulations closely matches experimental data up to approximately 1.5 GeV/c. However, in the range of 1.5−4 GeV/c, the v_2 values from AMPT begin to deviate from the data.
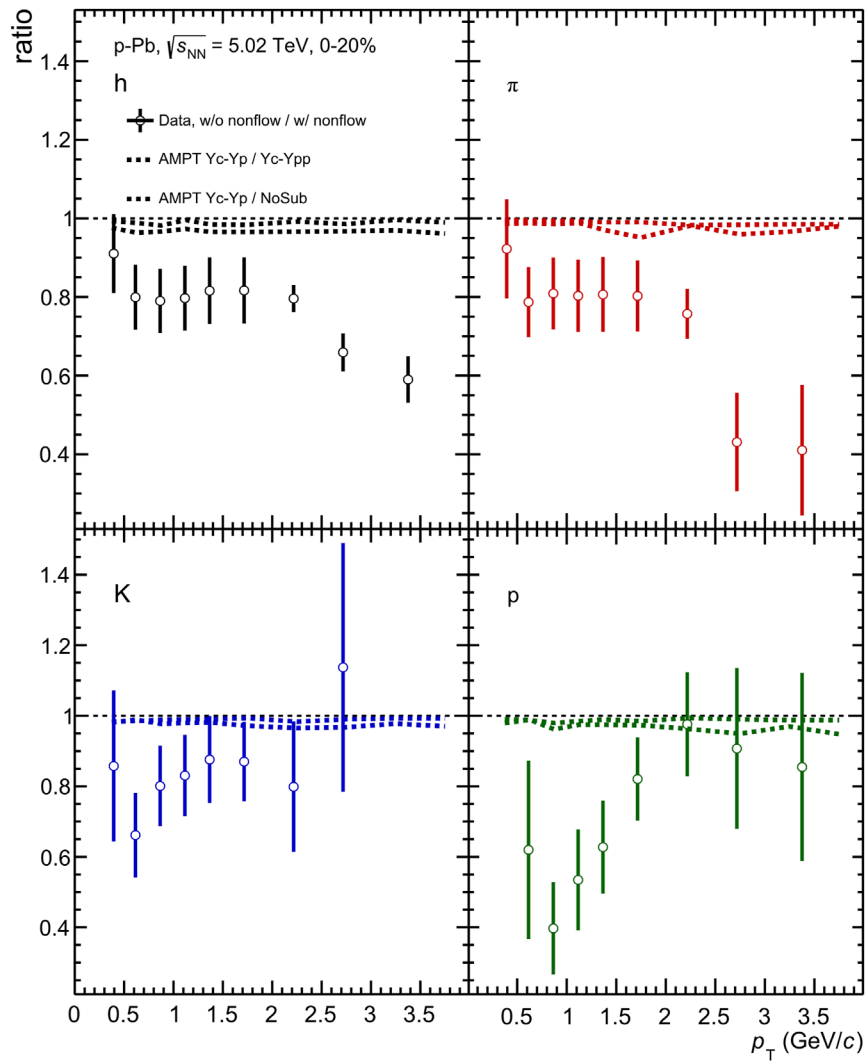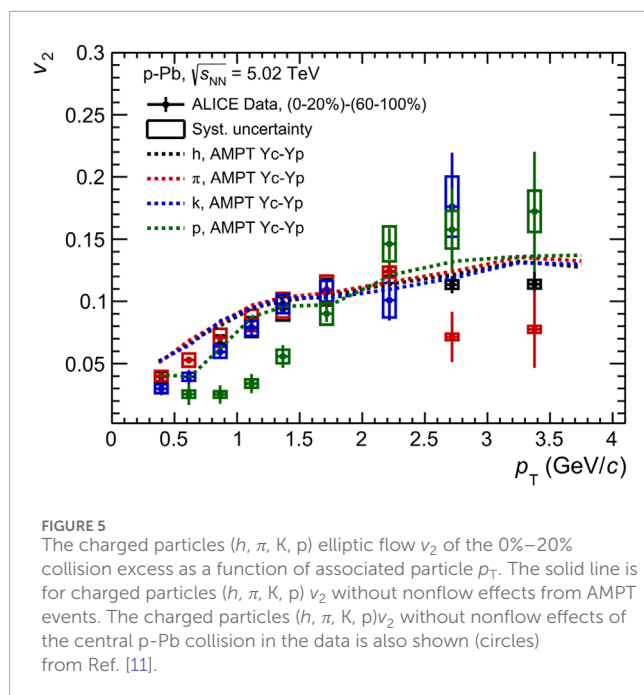
FIGURE 4
The ratio between charged particles (h, π, K, p) elliptic flow v_2 of most central collisions reduced by subtracting the per-trigger yield distribution in peripheral p-Pb collisions and pp collisions is shown by long dash-dotted line, the ratio between v_2 of most central p-Pb collisions reduced by subtracting the per-trigger yield distribution in peripheral p-Pb collisions and without nonflow subtracting is shown by short dash-dotted line. The ratio between charged particles (h, π, K, p) elliptic flow v_2 with and without nonflow contribution of the central p-Pb collision in the data is also shown (circles) from Ref. [11]. Error bars for data show statistical uncertainty and systematic uncertainty, added in quadrature.

In Figure 4, we can observe the ratio between charged particles (h, π, K, p) v_2 of most central p-Pb collisions reduced by subtracting the per-trigger yield distribution in peripheral p-Pb collisions and pp collisions is shown by long dash-dotted line, the maximum deviation is less than 2%. The ratio between v_2 of most central p-Pb collisions reduced by subtracting the per-trigger yield distribution in peripheral p-Pb collisions and without nonflow subtracting is shown by short dash-dotted line, the maximum deviation of ratio value is less than 5%. It is worth noting that the nonflow contribution can vary with p_T due to different physical mechanisms that contribute to particle production in different p_T ranges. For example, at low p_T, the nonflow contribution may be dominated by resonance decays, while at high p_T, the nonflow contribution may be dominated by

jet-like correlations. Therefore, studying the nonflow contribution ratio as a function of p_T can provide important insights into the underlying physics of particle production in heavy-ion collisions. When comparing AMPT events with experimental data, the ratio of v_2 values without nonflow effects to those with nonflow effects is similar for kaons, while it differs for charged particles, pions, protons, and antiprotons.

The charged particles (h, π, K, p) v_2 is shown as a function of associated p_T in Figure 5 at 0%–20% p-Pb collision centrality interval. We can find the second-order coefficients for pions and kaons are found to be comparable, while v_2^p is smaller than v_2^π at low p_T but becomes larger at high p_T, with a crossing point observed around 2 GeV/c.

FIGURE 5
The charged particles (h, π, K, p) elliptic flow v_2 of the 0%–20% collision excess as a function of associated particle p_T. The solid line is for charged particles (h, π, K, p) v_2 without nonflow effects from AMPT events. The charged particles (h, π, K, p)v_2 without nonflow effects of the central p-Pb collision in the data is also shown (circles) from Ref. [11].

5 Summary

In this study, we employ the multiphase transport model (AMPT) to comprehensively investigate the elliptic flow (v_2) of charged particles (h, π, K, p) in p-Pb collisions at $\sqrt{s_{NN}}$ = 5.02 TeV. Two-particle angular correlations of charged particles were calculated for these collisions and expressed as associated yields per trigger particle. The Fourier coefficient v_2 was extracted from the correlations and analyzed as a function of transverse momentum (p_T).

To reduce nonflow effects, such as jet correlations and resonance decays, in central p-Pb collisions, we subtracted the per-trigger yield distribution from peripheral p-Pb collisions or pp collisions at $\sqrt{s}$ = 5.02 TeV. Both methods yielded consistent results. We discuss comparisons with experimental measurements from p-Pb collisions at $\sqrt{s_{NN}}$ = 5.02 TeV, showing that nonflow effects in central p-Pb collisions are not strongly dependent on the choice of subtraction method.

With and without nonflow subtraction, the ratio of v_2 for the most central p-Pb collisions exhibits the maximum deviation being less than 5%. Analyzing the nonflow contribution as a function of p_T offers valuable insights into the physics of particle production in heavy-ion collisions. At low p_T, resonance decays likely dominate the nonflow contribution, while jet-like correlations become more significant at high p_T.

Furthermore, we compare our results with experimental data from p-Pb collisions at $\sqrt{s_{NN}}$ = 5.02 TeV. The ratio of v_2 values with and without nonflow subtraction is similar for kaons, but differs for other charged particles, pions, protons, and antiprotons. We observe that the second-order coefficients for pions and kaons are comparable, while v_2^p is smaller at low p_T and larger at high p_T compared to v_2^π, with a crossing point around 2 GeV/c.

Our results show that in p-Pb collisions, non-flow effects do not significantly depend on the yield of subtracting d-Au peripheral collisions or pp central collisions, which provides an important reference for subtracting nonflow contributions in small system collision experiments.

In the next step, based on the research method of this work, we will systematically study the influence of nonflow contribution on the higher-order flow coefficient v3 in d-Au collisions under the AMPT model, which can provide more theoretical references for researchers studying the reduction method of nonflow contribution in small collision systems.

Data availability statement

The original contributions presented in the study are included in the article/supplementary material, further inquiries can be directed to the corresponding authors.

Author contributions

NY: Data curation, Formal Analysis, Investigation, Methodology, Writing–original draft, Writing–review and editing, Software. ZZ: Formal Analysis, Writing–original draft, Writing–review and editing, Investigation. MZ: Writing–review and editing.

Funding

Acknowledgments

Conflict of interest

The authors declare that the research was conducted in the absence of any commercial or financial relationships that could be construed as a potential conflict of interest.

Generative AI statement

The author(s) declare that no Generative AI was used in the creation of this manuscript.

Publisher's note

All claims expressed in this article are solely those of the authors and do not necessarily represent those of their affiliated organizations, or those of the publisher, the editors and the reviewers. Any product that may be evaluated in this article, or claim that may be made by its manufacturer, is not guaranteed or endorsed by the publisher.

References

1. Muller B, Nagle JL. Results from the relativistic heavy ion collider. *Ann Rev Nucl Part Sci* (2006) 56:93–135. doi:10.1146/annurev.nucl.56.080805.140556

2. Bazavov A, et al. The chiral and deconfinement aspects of the QCD transition. *Phys Rev* (2012) D85:054503.

3. Ollitrault JY. Anisotropy as a signature of transverse collective flow. *Phys Rev D* (1992) 46:229–45. doi:10.1103/physrevd.46.229

4. Alver B, Roland G. Collision geometry fluctuations and triangular flow in heavy-ion collisions. *Phys.Rev.* (2010) C81:054905. doi:10.1103/physrevc.81.054905

5. Eskola KJ, Paukkunen H, Salgado CA. EPS09: a new generation of nlo and LO nuclear parton distribution functions. *JHEP* (2009) 04:065. doi:10.1088/1126-6708/2009/04/065

6. Kopeliovich BZ, Nemchik J, Schafer A, Tarasov AV. Cronin effect in hadron production off nuclei. *Phys Rev Lett* (2002) 88:232303. doi:10.1103/physrevlett.88.232303

7. Kang ZB, Vitev I, Wang E, Xing H, Zhang C. Multiple scattering effects on heavy meson production in p+A collisions at backward rapidity. *Phys Lett B* (2015) 740:23–9. doi:10.1016/j.physletb.2014.11.024

8. Collaboration CMS, Chatrchyan S, et al. Observation of long-range near-side angular correlations in proton-lead collisions at the LHC. *Phys Lett B* (2013) 718:795–814.

9. Collaboration ALICE, Abelev B, et al. Long-range angular correlations on the near and away side in pPb collisions at $\sqrt{s_{NN}}$ = 5.02 TeV TeV. *Phys Lett B* (2013) 719:29–41.

10. Collaboration ATLAS, Aad G, et al. Observation of associated near-side and away-side long-range correlations in $\sqrt{s_{NN}}$ = 5.02 TeV proton-lead collisions with the ATLAS detector. *Phys Rev Lett* (2013) 110(18):182302.

11. Collaboration ALICE, Abelev BB, et al. Long-range angular correlations of π, K and p in p–Pb collisions at $\sqrt{s_{NN}}$ = 5.02 TeV. *Phys Lett B* (2013) 726:164–77.

12. Collaboration ATLAS, Aaboud M, et al. Measurements of long-range azimuthal anisotropies and associated Fourier coefficients for pp collisions at $\sqrt{s_{NN}}$ = 5.02 and 13 TeV and p+Pb collisions at $\sqrt{s_{NN}}$ = 5.02 TeV with the ATLAS detector. *Phys Rev C* (2017) 96(2):024908.

13. Zhang ZM, Li S, Yu N, Wu Q. Investigating nonflow contribution subtraction in d-Au collisions with AMPT model. *Eur Phys J A* (2023) 59:130. doi:10.1140/epja/s10050-023-01038-z

14. Collaboration LHC, Aaij R, et al. Measurements of long-range near-side angular correlations in $\sqrt{s_{NN}}$ = 5 TeV proton-lead collisions in the forward region. *Phys Lett B* (2016) 762:473–83.

15. Collaboration PHENIX, Adare A, et al. Quadrupole anisotropy in dihadron azimuthal correlations in central d + Au collisions at $\sqrt{s_{NN}}$ = 200 GeV. *Phys Rev Lett* (2013) 111(21):212301.

16. Collaboration PHENIX, Adare A, et al. Measurement of long-range angular correlation and quadrupole anisotropy of pions and (anti)protons in central d + Au collisions at $\sqrt{s_{NN}}$ = 200 GeV. *Phys Rev Lett* (2015) 114(19):192301.

17. Collaboration STAR, Adamczyk L, et al. "Long-range pseudorapidity dihadron correlations in d+Au collisions at $\sqrt{s_{NN}}$ = 200 GeV", *Phys Lett B* 747 (2015) 265–71.

18. PHENIX Collaboration, Adare A, Aidala C, Ajitanand NN, Akiba Y, Akimoto R, et al. Measurements of elliptic and triangular flow in high-multiplicity ³He+Au collisions at $\sqrt{s_{NN}}$ = 200 GeV. *Phys Rev Lett* (2015) 115(14):142301. doi:10.1103/PhysRevLett.115.142301

19. Collaboration ATLAS, Aad G, et al. Measurement of long-range pseudorapidity correlations and azimuthal harmonics in $\sqrt{s_{NN}}$ = 5.02 TeV proton-lead collisions with the ATLAS detector. *Phys Rev C* (2014) 90(4):044906.

20. Pack V, f or the ALICE Collaboration). Elliptic flow of identified hadrons in small collisional systems measured with ALICE. *Nucl.Phys A* (2019) 982:451–4.

21. Aad G, Abbott DC, Abud AA, Abeling K, Abhayasinghe DK, et al. Transverse momentum and process dependent azimuthal anisotropies in $\sqrt{s_{NN}}$ = 8.16 TeV p+Pb collisions with the ATLAS detector. *Eur Phys J C* (2020) 80(1):73. doi:10.1140/epjc/s10052-020-7624-4

22. Lin ZW, Ko CM, Li BA, Zhang B, Pal S. Multiphase transport model for relativistic heavy ion collisions. *Phys Rev C* (2005) 72:064901. doi:10.1103/physrevc.72.064901

23. Wang XN, Gyulassy M. hijing: a Monte Carlo model for multiple jet production in pp, pA, and AA collisions. *Phys Rev D* (1991) 44:3501–16. doi:10.1103/physrevd.44.3501

24. Zhang B. ZPC 1.0.1: a Parton cascade for ultrarelativistic heavy ion collisions. *Comput Phys Commun* (1998) 109:193–206. doi:10.1016/s0010-4655(98)00010-1

25. Li BA, Ko CM. Formation of superdense hadronic matter in high-energy heavy ion collisions. *Phys Rev C* (1995) 52:2037–63. doi:10.1103/physrevc.52.2037

26. Voloshin S, Zhang Y. Flow study in relativistic nuclear collisions by Fourier expansion of Azimuthal particle distributions. *Z Phys C* (1996) 70:665–71. doi:10.1007/s002880050141

27. Zheng L, Li H, Qin H, Shou QY, Yin ZB. Investigating the NCQ scaling of elliptic flow at LHC with a multiphase transport model. *Eur Phys J* (2017) A 53:124. doi:10.1140/epja/i2017-12312-8

28. Adam J, et al. Forward-central two-particle correlations in p–Pb collisions at $\sqrt{s_{NN}}$ = = 5.02 TeV. *Phys Lett B* (2016) 753:126–39.

29. Acharya S, et al. Search for collectivity with azimuthal J/ψ-hadron correlations in high multiplicity p–Pb collisions at $\sqrt{s_{NN}}$ = 5.02 and 8.16 TeV. *Phys Lett B* (2018) 780:7–20.

30. Collaboration ALICE, Acharya S, et al. Azimuthal anisotropy of heavy-flavor decay electrons in p-Pb collisions at $\sqrt{s_{NN}}$ = 5.02 TeV. *Phys Rev Lett* (2019) 122(7):072301.

31. Lim SH, Hu Q, Belmont R, Hill KK, Nagle JL, Perepelitsa DV. Examination of flow and nonflow factorization methods in small collision systems. *Phys Rev C* (2019) 100:024908. doi:10.1103/physrevc.100.024908

32. Luzum M. Collective flow and long-range correlations in relativistic heavy ion collisions. *Phys Lett B* (2011) 696:499–504. doi:10.1016/j.physletb.2011.01.013